Electronic Supplementary Material (ESI) for Journal of Materials Chemistry A.

Electronic Supplementary Information

Charge Separation in Hybrid Metal-Organic Framework Films for Enhanced Catalytic CO_2 Conversion

Yi Guo,[a,b] Bin Gao,[a,c] Zheng Deng,[b] Yu Liu,[a,d] Xinsheng Peng,*,[b] Yanli Zhao*,[a]

[a] Division of Chemistry and Biological Chemistry, School of Physical and Mathematical Sciences, Nanyang Technological University, 21 Nanyang Link, 637371, Singapore

[b] State Key Laboratory of Silicon Materials, School of Materials Science and Engineering, Zhejiang University, Hangzhou, 310027, China

[c] College of Materials Science and Technology, Jiangsu Key Laboratory of Electrochemical Energy Storage Technologies, Nanjing University of Aeronautics and Astronautics, 211106, Nanjing, China

[d] Tianjin Key Laboratory of Structure and Performance for Functional Molecules, Key Laboratory of Inorganic-Organic Hybrid Functional Material Chemistry (Ministry of Education), College of Chemistry, Tianjin Normal University, Tianjin, 300387, China

Email: zhaoyanli@ntu.edu.sg, pengxinsheng@zju.edu.cn

Materials and chemicals:

2-Aminoethanol (NH_2-CH_2CH_2OH, AE), copper nitrate ($Cu(NO_3)_2$•$3H_2O$), N,N-dimethylformamide (DMF), and [6,6]-phenyl C_{61} butyric acid methyl ester ($PC_{61}BM$) were purchased from Sigma-Aldrich. Epichlorohydrin, 1,2-epoxybutane, propylene oxide, styrene oxide, tetrabutylammonium bromide (TBAB), and *meso*-tetra(4-carboxyphenyl)porphine (TCPP) were purchased from Tokyo Chemical Industry Co., Ltd. Acetonitrile (CH_3CN), ethanol, and toluene were purchased from Fisher Scientific Co. Ltd. Acetonitrile-d_3 (CD_3CN) was purchased from Cambridge Isotope Laboratories, Inc. Polycarbonate (PC) membranes (Whatman) with an average pore size of 200 nm were employed for the filtration. Ultrapure water of 18.2 MΩ produced by a Millipore direct-Q system was used throughout the experiments.

Synthesis of $PC_{61}BM$/CuTCPP films:

Copper hydroxide nanostrands (CHNs) were synthesized as reported previously.[1,2] AE aqueous solution (1.4 mM) was quickly mixed with equal volume $Cu(NO_3)_2$ aqueous solution under stirring and aged at ambient temperature for at least 12 h to form CHN colloidal solution. $PC_{61}BM$ toluene solution (12.5, 25, 50, 75 or 100 μL of 1 mg/mL) was dispersed into methanol (5 mL), and then the mixture was poured into CHNs solution (15 mL) under stirring for 1 min. The $PC_{61}BM$/CHNs composite film was obtained by filtering the fore-mentioned mixture solution onto PC membrane followed by transferring it onto glass with the assistance of ethanol. Subsequently, CHNs/$PC_{61}BM$ film was placed in 0.5 mM TCPP DMF/ethanol (volume ratio, 3/1) solution and heated at 65 ºC for 24 h. $PC_{61}BM$/CuTCPP film was successfully prepared and named as $PC_{61}BM$/CuTCPP-0.4%, $PC_{61}BM$/CuTCPP-0.9%, $PC_{61}BM$/CuTCPP-1.8%, $PC_{61}BM$/CuTCPP-2.7% and $PC_{61}BM$/CuTCPP-3.5%, respectively. After washing with DMF/ethanol (volume ratio, 3/1) solution for 3 times and drying, $PC_{61}BM$/CuTCPP films were ready for the following tests.

To prepare $PC_{61}BM$/CuTCPP film with different thickness, $PC_{61}BM$ toluene solution (100 and 150 μL, 1 mg/mL) was dispersed into methanol (5 mL), and then the mixture was poured into CHN solution (30 and 45 mL) under stirring for 1 min. The mixture was filtered to obtain $PC_{61}BM$/CHNs composite film. After soaking in 0.5 mM TCPP DMF/ethanol (volume ratio, 3/1) solution and heated at 65 ºC for 24 h, $PC_{61}BM$/CHNs composite film was converted to $PC_{61}BM$/CuTCPP composite film with thickness of 6 μm and 11 μm, respectively.

Characterizations:

The morphologies of the as-prepared films were characterized by scanning electronic microscopy (SEM) (JSM-7600F). The phase of the films was recorded by powder X-ray diffraction (XRD) at 0.02 degree step using Rigaku MiniFlex 600 with Cu Kα radiation. Fourier transform infrared (FT-IR) spectroscopy was measured by Shimadzu IRAffinity-1S using a KBr pellet in a range of 600-2000 cm^{-1}. Raman spectra were recorded by Thermo Fisher Scientific DXR Raman Microscope. Thermogravimetric analysis (TGA) was conducted on TA-Q500 under N_2 atmosphere. Zeta potentials of CHNs and $PC_{61}BM$ were characterized by Zetadizer3000HSA. XPS and UPS were measured through SPECSLab and Kratos SUPRA. Photoluminescence (PL) spectra of PC_{61} BM/CuTCPP films were measured on Shimadzu RF-5301PC with exciting light of 350 nm.

Electrochemical characterization:

The working electrode was $PC_{61}BM$/CuTCPP film on ITO glass. The electrochemical measurements were conducted on CHI 760e electrochemical workstation, with Pt plate as the counter electrode and saturated calomel electrode. The tests were performed in phosphatic buffer solution (pH=7) at room temperature.

Photocatalysis experiments:

The CO_2 conversion reaction was conducted in a Schlaker reaction tube. The as-prepared film (1 mg) was soaking in epoxide solution (1.5 mL) with CH_3CN as solvent. The epoxide concentration was fixed as 1 mmol/1.5 mL. TBAB was employed as co-catalyst with weight of 0.0325g. A CO_2 balloon was connected to Schlaker reaction tube to purge CO_2 into the reaction system at 1 atm. Then, the system was placed under Xeon lamp (Perfectlight, 100 mW/cm^2, 400 nm $< \lambda <$ 800 nm) for several hours. The cycloaddition products were calculated based on ^1H NMR analysis (Bruker Avance 300).

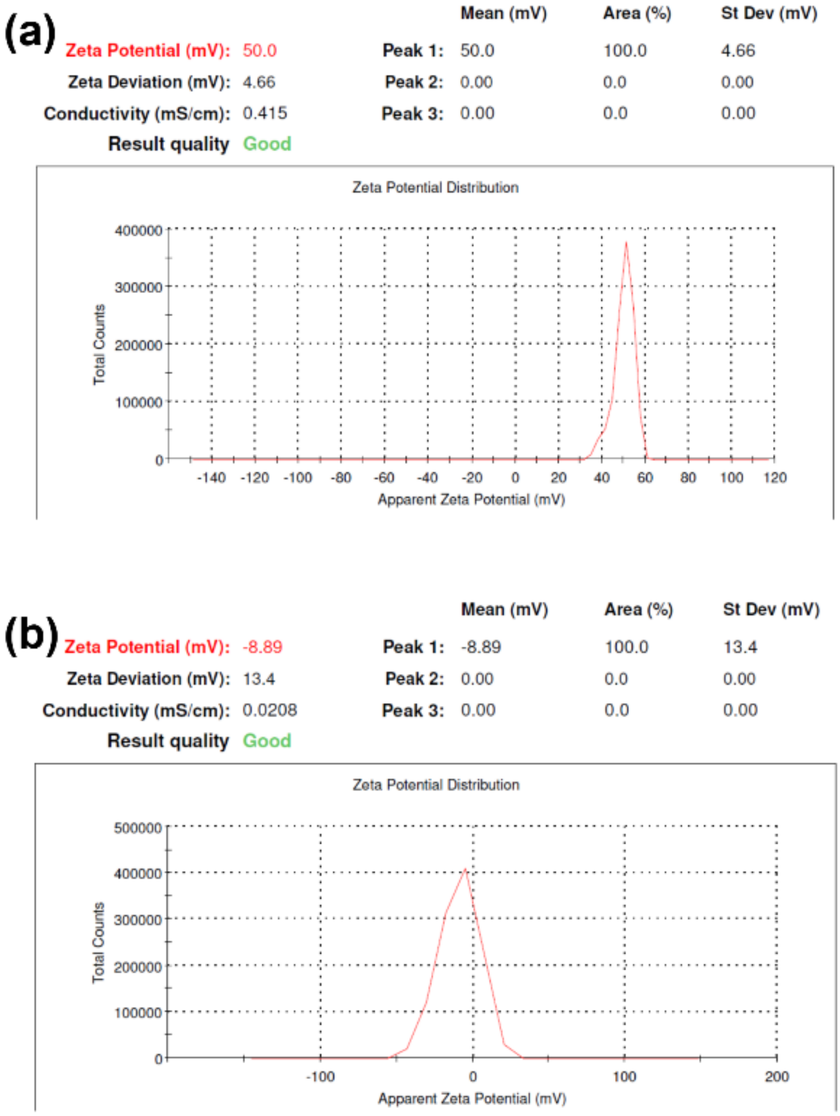

(a)

Zeta Potential (mV): 50.0
Zeta Deviation (mV): 4.66
Conductivity (mS/cm): 0.415
Result quality Good

	Mean (mV)	Area (%)	St Dev (mV)
Peak 1:	50.0	100.0	4.66
Peak 2:	0.00	0.0	0.00
Peak 3:	0.00	0.0	0.00

(b)

Zeta Potential (mV): -8.89
Zeta Deviation (mV): 13.4
Conductivity (mS/cm): 0.0208
Result quality Good

	Mean (mV)	Area (%)	St Dev (mV)
Peak 1:	-8.89	100.0	13.4
Peak 2:	0.00	0.0	0.00
Peak 3:	0.00	0.0	0.00

Figure S1. Zeta potential of (a) CHNs and (b) $PC_{61}BM$.

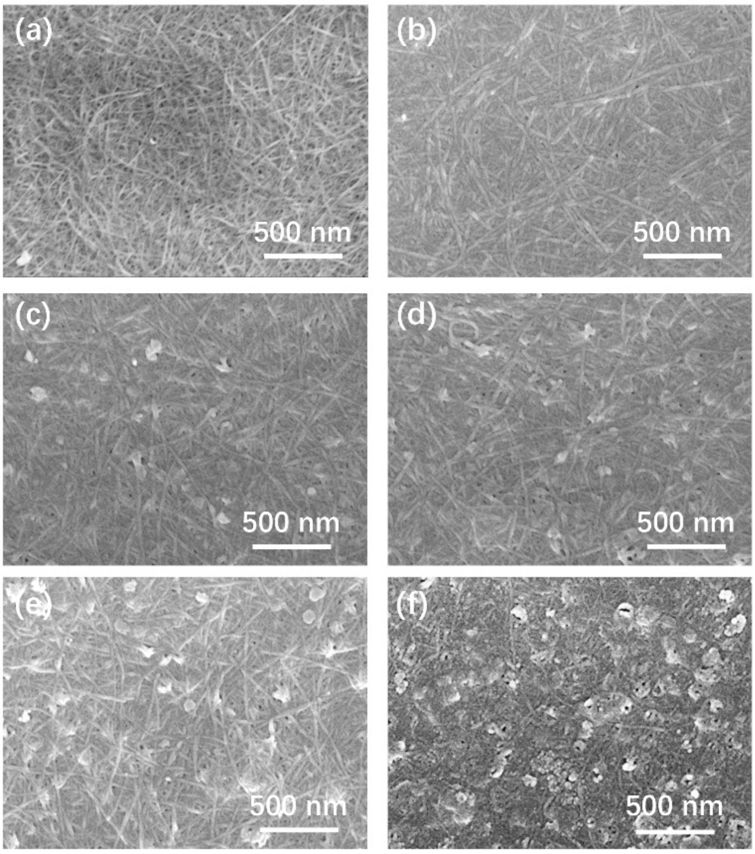

Figure S2. SEM images for surface of (a) CHNs film, (b) CHNs/PC$_{61}$BM-0.4% film, (c) CHNs/PC$_{61}$BM-0.9% film, (d) CHNs/PC$_{61}$BM-1.8% film, (e) CHNs/PC$_{61}$BM-2.7%, and (f) CHNs/PC$_{61}$BM-3.5% film.

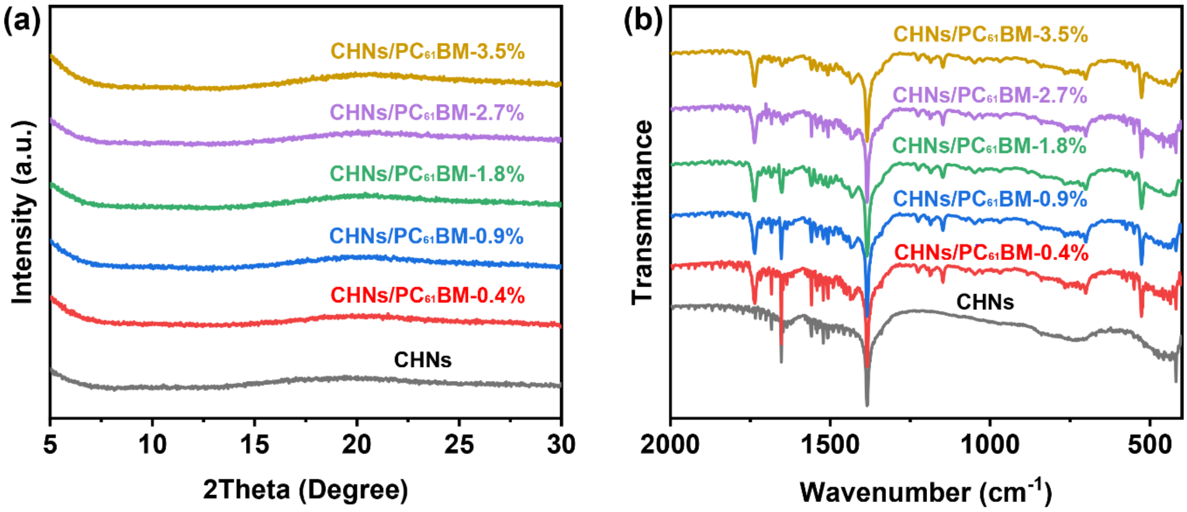

Figure S3. (a) Powder XRD patterns and (b) FTIR spectra of CHNs/PC$_{61}$BM films.

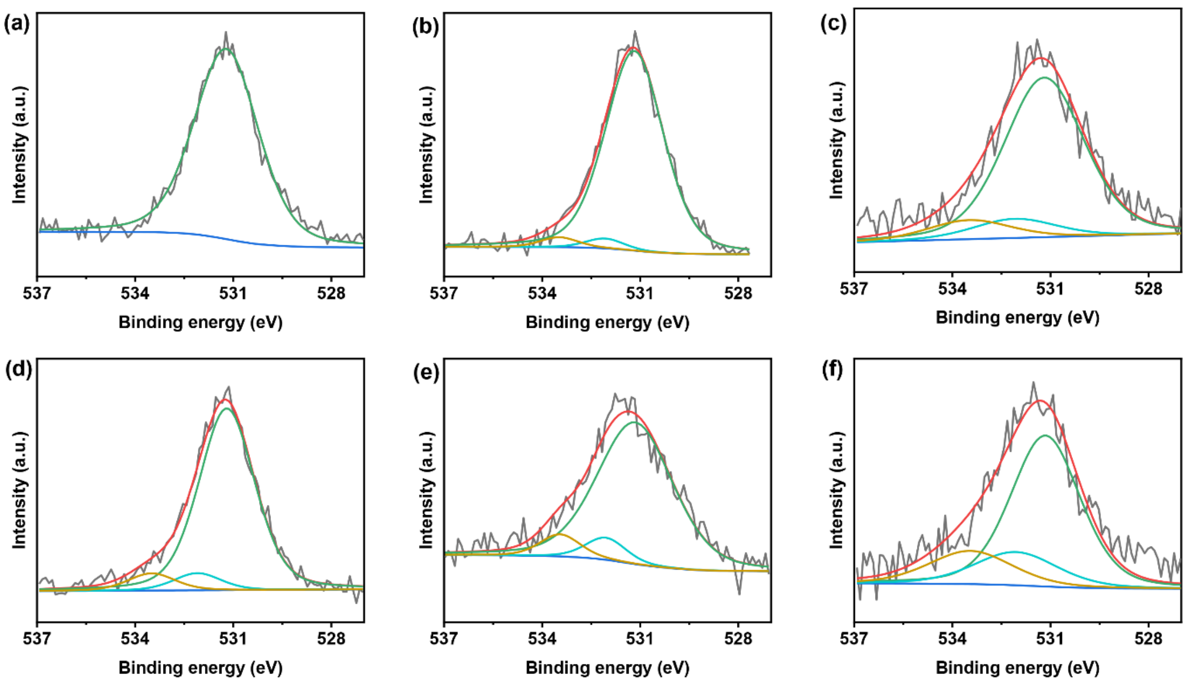

Figure S4. XPS O1s spectra of (a) CHNs, (b) CHNs/$PC_{61}BM$-0.4%, (c) CHNs/$PC_{61}BM$-0.9%, (d) CHNs/$PC_{61}BM$-1.9%, (e) CHNs/$PC_{61}BM$-2.7%, and (f) CHNs/$PC_{61}BM$-3.5%.

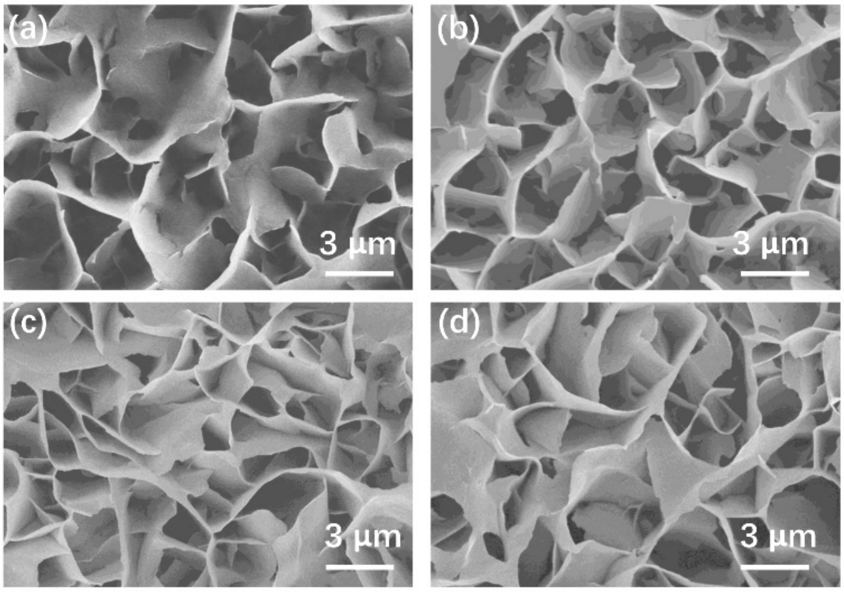

Figure S5. SEM images for surface of (a) $PC_{61}BM$/CuTCPP-0.4% film, (b) $PC_{61}BM$/CuTCPP-0.9% film, (c) $PC_{61}BM$/CuTCPP-2.7% film, and (d) $PC_{61}BM$/CuTCPP-3.5% film.

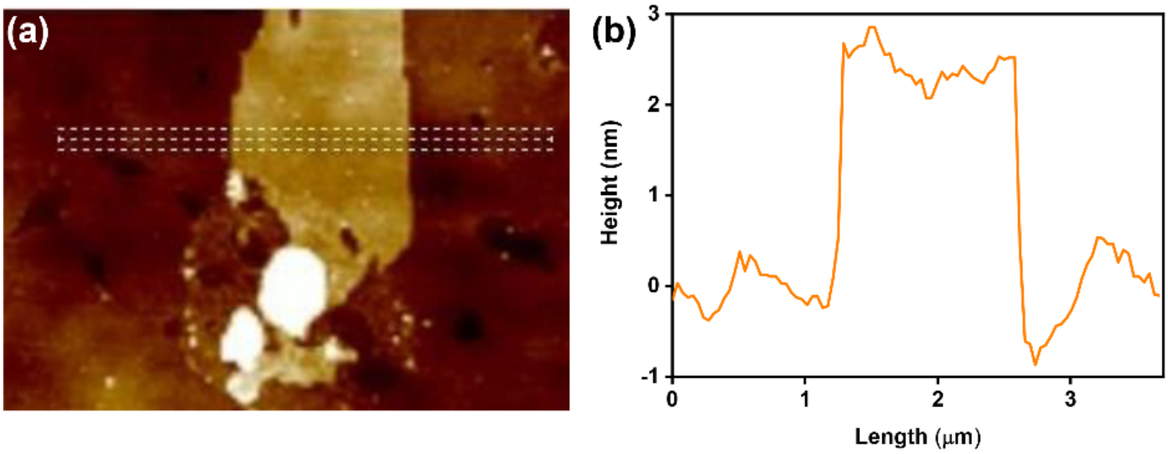

Figure S6. (a) AFM image of 2D $PC_{61}BM$/CuTCPP-1.8% sheet. (b) Height of $PC_{61}BM$/CuTCPP-1.8% sheet.

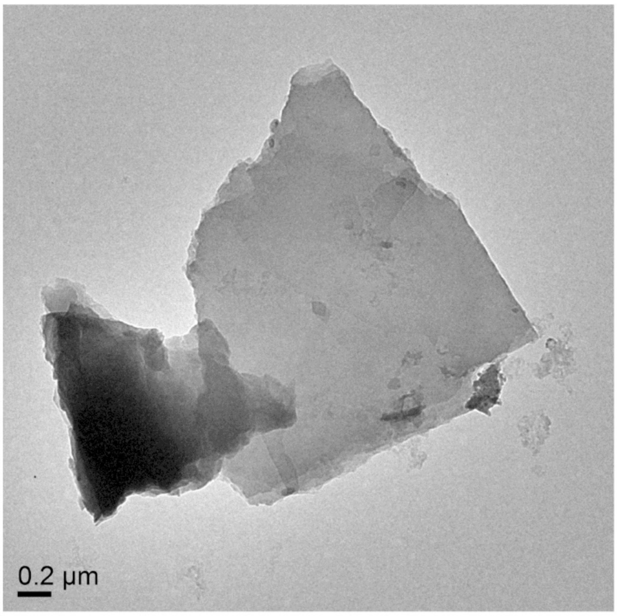

Figure S7. TEM image of $PC_{61}BM$/CuTCPP-1.8% sheet.

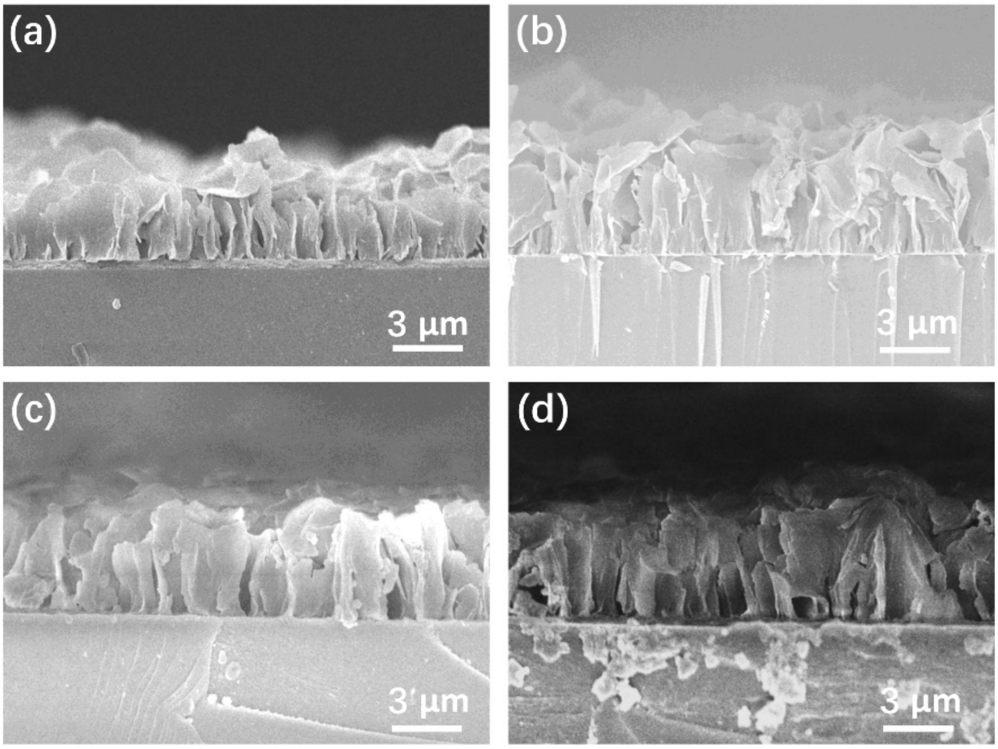

Figure S8. SEM images for cross-section of (a) $PC_{61}BM$/CuTCPP-0.4% film, (b) $PC_{61}BM$/CuTCPP-1.8% film, (c) $PC_{61}BM$/CuTCPP-2.7% film, and (d) $PC_{61}BM$/CuTCPP-3.5% film.

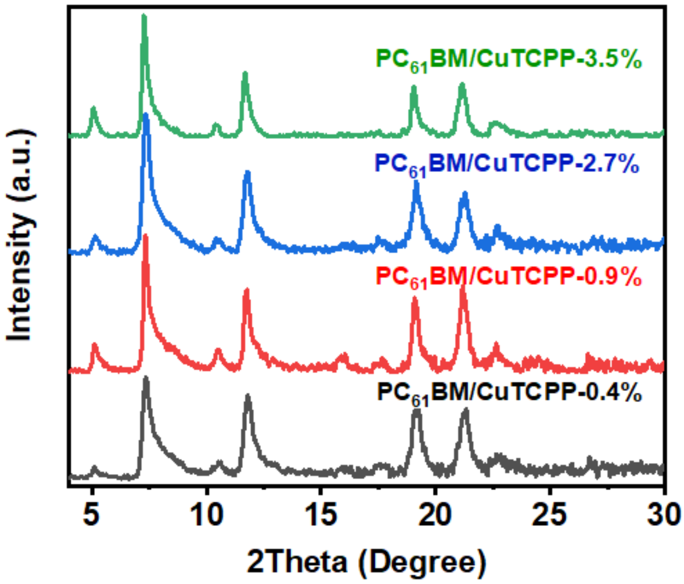

Figure S9. Powder XRD patterns of $PC_{61}BM$/CuTCPP films with various $PC_{61}BM$ concentrations.

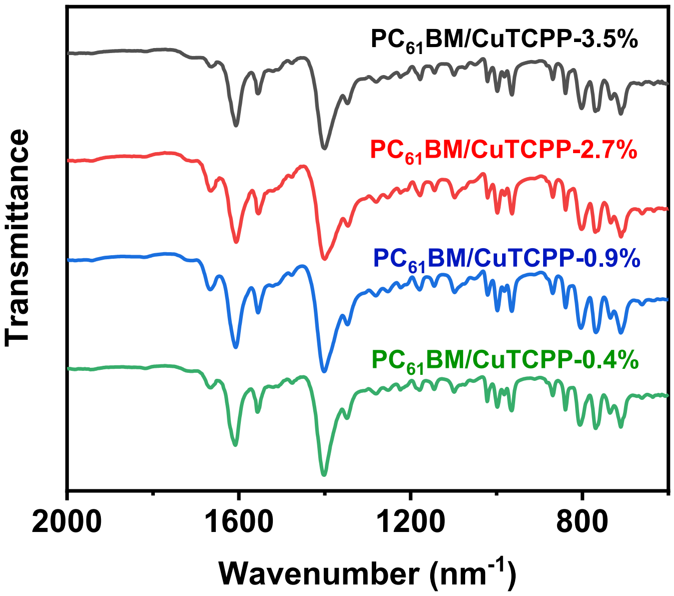

Figure S10. FT-IR spectra of $PC_{61}BM$/CuTCPP films with various $PC_{61}BM$ concentrations.

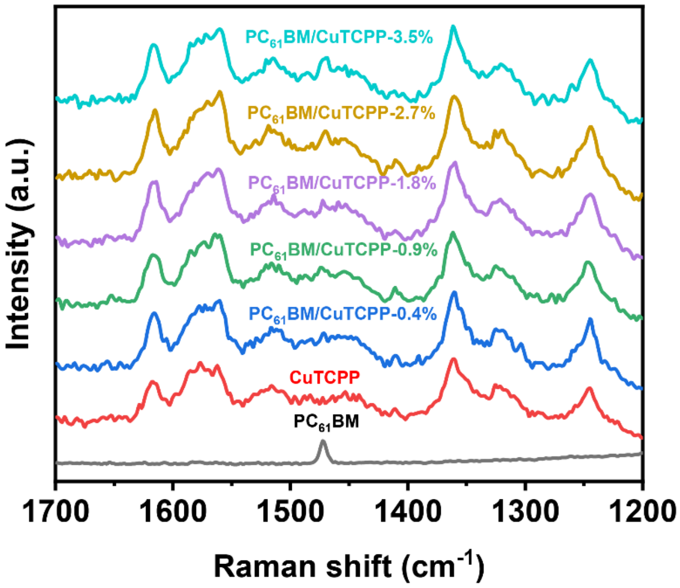

Figure S11. Raman spectra of $PC_{61}BM$/CuTCPP films with various $PC_{61}BM$ concentrations.

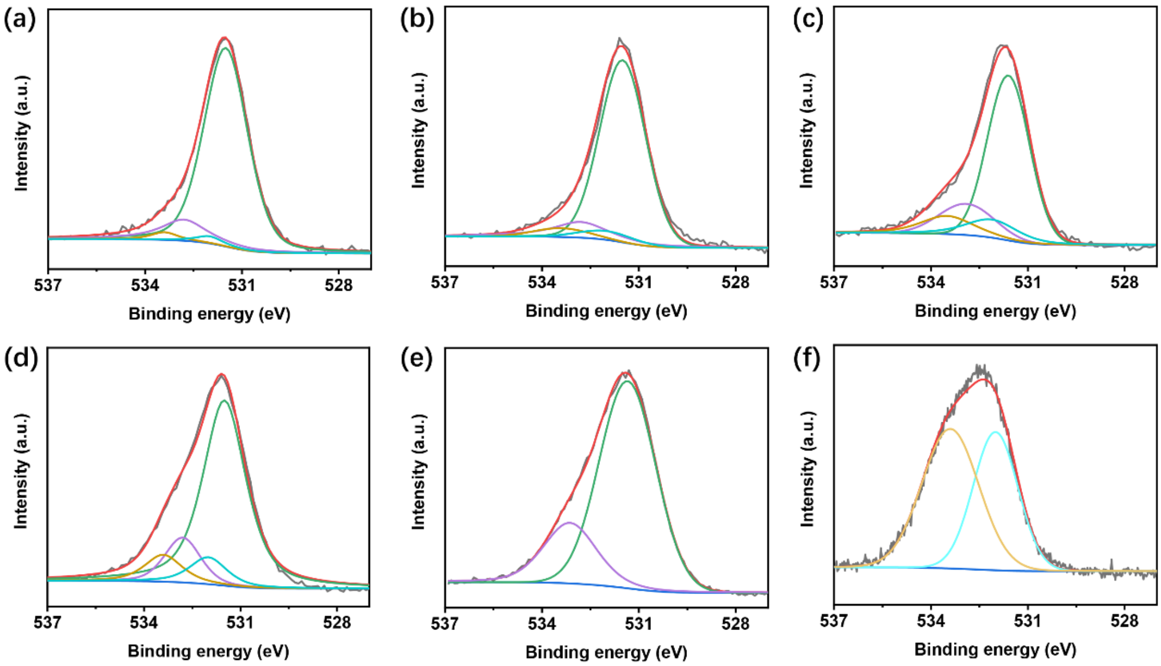

Figure S12. XPS O1s spectra of (a) PC61BM/CuTCPP-0.4% film, (b) PC61BM/CuTCPP-0.9% film, (c) PC61BM/CuTCPP-2.7% film, (d) PC61BM/CuTCPP-3.5% film, (e) CuTCPP film, and (f) PC61BM.

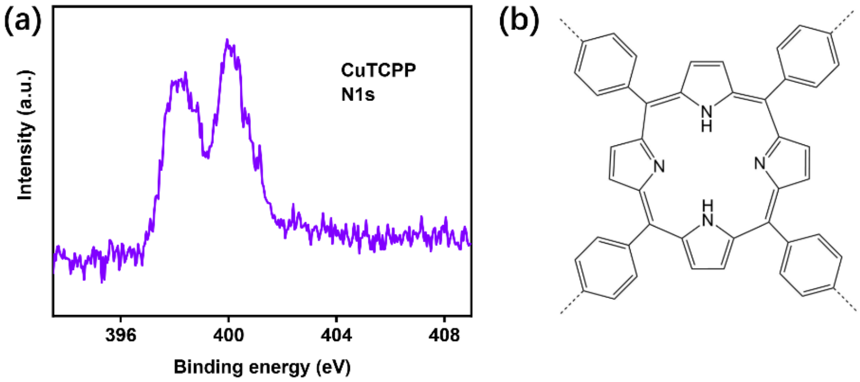

Figure S13. (a) XPS N1s spectrum of CuTCPP film. The two major peaks indicate that there are two status N atoms, as shown in (b).

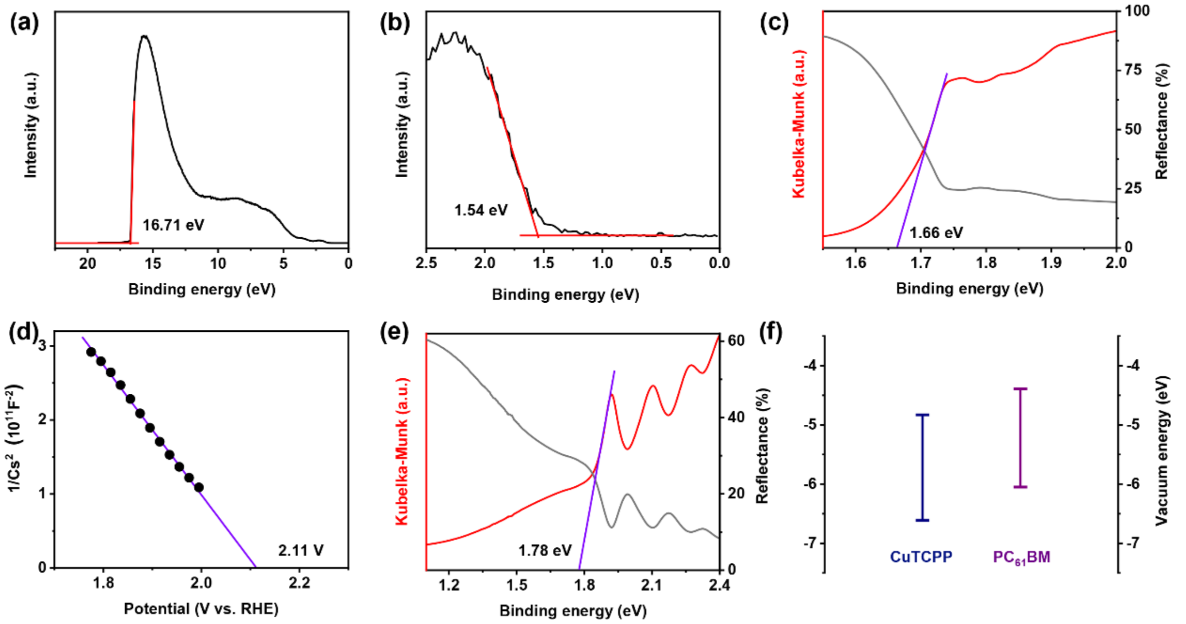

Figure S14. (a) UPS, (b) VBM and (c) UV-vis-DRS of $PC_{61}BM$. (d) Mott-Schottky plot and (e) UV-vis-DRS of CuTCPP film. (f) Band structures of $PC_{61}BM$ and CuTCPP film.

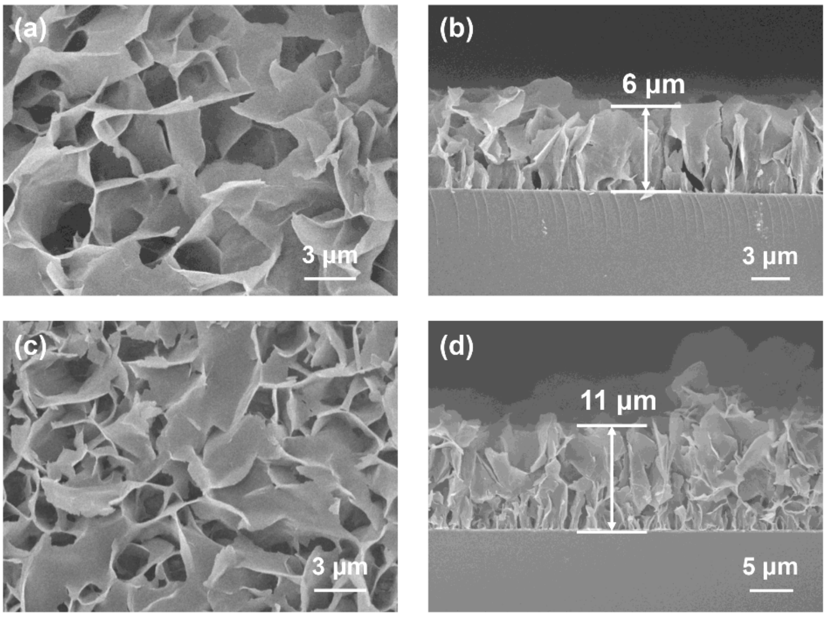

Figure S15. SEM images of (a) surface and (b) cross-section of $PC_{61}BM$/CuTCPP-1.8%-6 μm, and (c) surface and (d) cross-section of $PC_{61}BM$/CuTCPP-1.8%-11 μm.

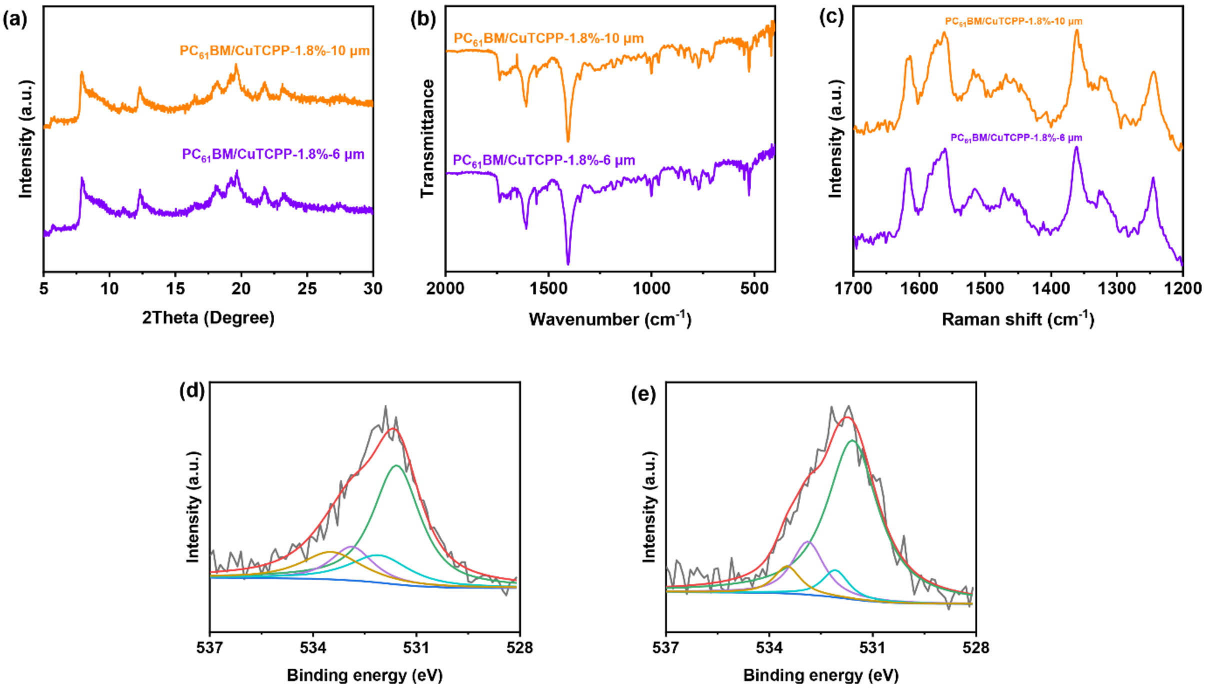

Figure S16. (a) Powder XRD patterns, (b) FTIR spectra, and Raman spectra of PC$_{61}$BM/CuTCPP-1.8%-6 μm and PC$_{61}$BM/CuTCPP-1.8%-11 μm. XPS O1s spectra of (d) PC$_{61}$BM/CuTCPP-1.8%-6 μm and (e) PC$_{61}$BM/CuTCPP-1.8%-11 μm.

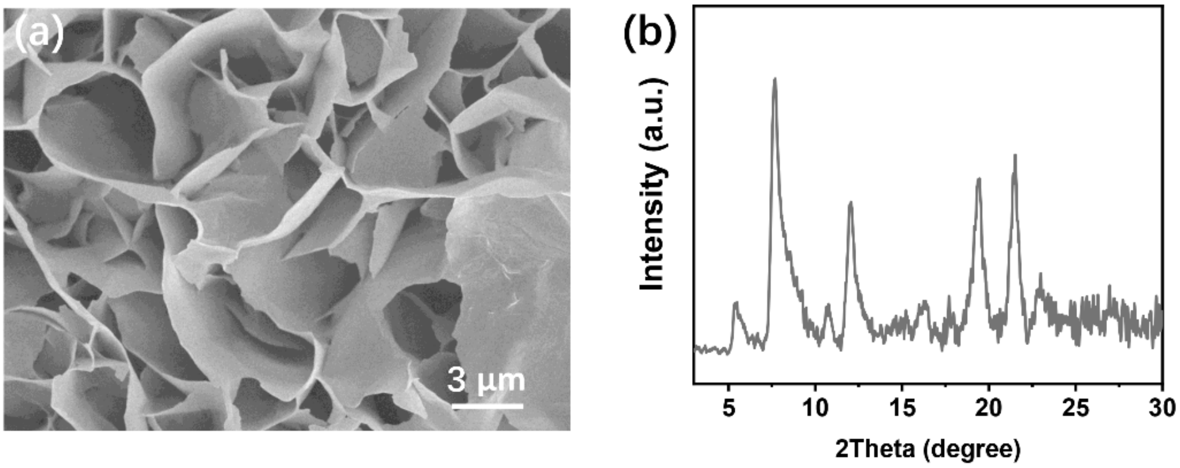

Figure S17. (a) SEM image and (b) powder XRD pattern of PC$_{61}$BM/CuTCPP-1.8% film after the catalysis.

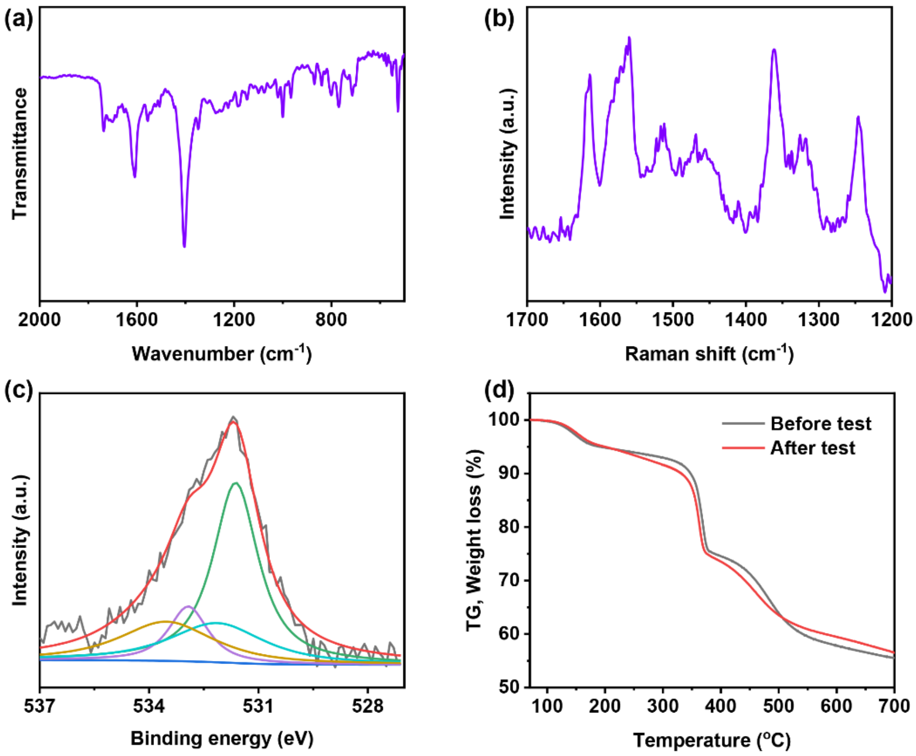

Figure S18. (a) FTIR spectrum, (b) Raman spectrum, (c) XPS O1s spectrum, and (d) TGA curve of $PC_{61}BM$/CuTCPP-1.8% film after the catalysis.

Table S1. Cycloaddition of CO_2 with epoxides catalyzed by $PC_{61}BM$/CuTCPP-1.8% film with various thickness.

Catalyst	Epoxide	Product	Conversion (%)	TOF (h^{-1})
$PC_{61}BM$/CuTCPP-1.8%-6 μm	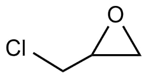	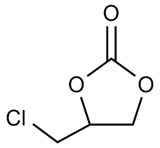	91.2	32.4
$PC_{61}BM$/CuTCPP-1.8%-11 μm	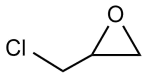	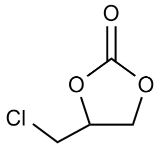	93.2	34.1

Table S2. Catalysis performance of MOF-based catalysts on the CO_2 cycloaddition with epichlorohydrin.

	Catalyst	T (ºC)	CO_2 pressure (bar)	Conversion (%)	TOF (h^{-1})	Ref.
1	$\{[Ni_4L(\mu_3\text{-}OH)_2(H_2O)_6]\cdot 2(H_2O)\cdot DMA\}_n$	100	10	99	1320	S3
2	MOF-Zn-1	100	10	97	83.25	S4
3	Zn(PZDC)(ATZ)	90	10	98	33.81	S5
4	MIL-101-tzmOH-Br	80	10	97	18	S6
5	Ni@UiO-66-NH_2	70	10	96.61	46	S7
6	mesoCu@Al-bpydc	60	10	98.7	5.88	S8
7	Zn(Bmic)(AT)	80	5	98	30.1	S9
8	JLU-LiuU21	35	1.5	99	4.74	S10
9	ZnTCPP$\subset$(Br^-)Etim-UiO-66	140	1	86.9	6.53	S11
10	$\{(Me_2NH_2)_2\cdot[Zn_8(Ad)_4(DABA)_6O]\cdot 7DMF\}_n$	100	1	99	50.4	S12
11	$[Zn_2(TCA)(BIB)_{2.5}]\cdot(NO_3)$	80	1	99	49.5	S13
12	Co-MOF	80	1	93	31	S14
13	FJI-H14	80	1	95	8.25	S15
14	MIL-101(Cr)	80	1	92	7.67	S16
15	$(\{[Ni_3Th_6(m_3\text{-}O)_4(m_3\text{-}OH)_4(IN)_{12})(H_2O)_{12}]\cdot(OH)_6\cdot 5DMF\cdot 2H_2O\}_n$	70	1	99	3.3	S17
16	FJI-C10	60	1	87	20.58	S18
17	MIL-101-IP	50	1	99	2.5	S19
18	$\{Na[Zn_{1.5}(\mu_4\text{-}O)(L)]\}_n$	50	1	98	1.63	S20
19	CuMOF	25	1	85	8.85	S21
20	Cu_2L_1	25	1	88	9.17	S22
21	$PC_{61}BM$/CuTCPP-1.8%	25	1	92.4	36.0	This work

References

(S1) Y. Guo, Y. Ying, Y. Mao, X. Peng and B. Chen, *Angew. Chem. Int. Ed.* 2016, **55**, 15120.

(S2) Y. Mao, J. Li, W. Cao, Y. Ying, P. Hu, Y. Liu, L. Sun, H. Wang, C. Jin and X. Peng, *Nat. Commun.* 2014, **5**, 5532.

(S3) C. Y. Gao, Y. Yang, J. H. Liu and Z. M. Sun, *Dalton Trans.* 2019, **48**, 1246.

(S4) J. W. Lan, M. S. Liu, X. Y. Lu, X. Zhang and J. M. Sun, *ACS Sustain. Chem. Eng.* 2018, **6**, 8727.

(S5) Y. X. Li, X. Zhang, P. Xu, Z. M. Jiang and J. M. Sun, *Inorg. Chem. Front.* 2019, **6,** 317.

(S6) L. J. Zhou, W. Sun, N. N. Yang, P. Li, T. Gong, W. J. Sun, Q. Sui and E. Q. Gao, *ChemSusChem* 2019, **12**, 2202.

(S7) M. Singh, P. Solanki, P. Patel, A. Mondal and S. Neogi, *Inorg. Chem.* 2019, **58**, 8100.

(S8) G. G. Chang, X. C. Ma, Y. X. Zhang, L. Y. Wang, G. Tian, J. W. Liu, J. Wu, Z. Y. Hu, X. Y. Yang and B. L. Chen, *Adv. Mater.* 2019, **31**, 1904969.

(S9) Y. X. Li, X. Zhang, J. W. Lan, P. Xu and J. M. Sun, *Inorg. Chem.* 2019, **58**, 13917.

(S10) J. Gu, X. Sun, X. Liu, Y. Yuan, H. Shan and Y. Liu, *Inorg. Chem. Front.* 2020, **7**, 4517.

(S11) J. Liang, Y. Q. Xie, Q. Wu, X. Y. Wang, T. T. Liu, H. F. Li, Y. B. Huang and R. Cao, *Inorg. Chem.* 2018, **57**, 2584.

(S12) H. M. He, Q. Q. Zhu, J. N. Zhao, H. M. Sun, J. Chen, C. P. Li and M. Du, *Chem. Eur. J.* 2019, **25**, 11474.

(S13) C. Yao, S. L. Zhou, X. J. Kang, Y. Zhao, R. Yan, Y. Zhang and L. L. Wen, *Inorg. Chem.* 2018, **57**, 11157.

(S14) B. Ugale, S. Kumar, T. J. D. Kumar and C. M. Nagaraja, *Inorg. Chem.* 2019, **58**, 3925.

(S15) L. F. Liang, C. P. Liu, F. L. Jiang, Q. H. Chen, L. J. Zhang, H. Xue, H. L. Jiang, J. J. Qian, D. Q. Yuan and M. C. Hong, *Nat. Commun.* 2017, **8,** 1233.

(S16) E. Akimana, J. Wang, N. V. Likhanova, S. Chaemchuen and F. Verpoort, *Catalysts* 2020, **10**, 453.

(S17) H. Xu, C. S. Cao, H. S. Hu, S. B. Wang, J. C. Liu, P. Cheng, N. Kaltsoyannis, J. Li and B. Zhao, *Angew. Chem. Int. Ed.* 2019, **58**, 6022.

(S18) J. Liang, Y. Q. Xie, X. S. Wang, Q. Wang, T. T. Liu, Y. B. Huang and R. Cao, *Chem. Commun.* 2018, **54**, 342.

(S19) B. Aguila, Q. Sun, X. L. Wang, E. O'Rourke, A. M. Al-Enizi, A. Nafady and S. Q. Ma, *Angew. Chem. Int. Ed.* 2018, **57**, 10107.

(S20) W. Z. Qiao, T. Q. Song and B. Zhao, *Chinese J. Chem.* 2019, **37**, 474.

(S21) P. Z. Li, X. J. Wang, J. Liu, J. S. Lim, R. Q. Zou and Y. L. Zhao, *J. Am. Chem. Soc.* 2016, **138**, 2142.

(S22) P. Z. Li, X. J. Wang, J. Liu, H. S. Phang, Y. X. Li and Y. L. Zhao, *Chem. Mater.* 2017, **29**, 9256.